



# Impact of a future H<sub>2</sub>-based road transportation sector on the composition and chemistry of the atmosphere – Part 2: Stratospheric ozone

D. Wang<sup>1</sup>, W. Jia<sup>1</sup>, S. C. Olsen<sup>1</sup>, D. J. Wuebbles<sup>1</sup>, M. K. Dubey<sup>2</sup>, and A. A. Rockett<sup>3</sup>

<sup>1</sup>Department of Atmospheric Sciences, University of Illinois at Urbana-Champaign, Urbana, IL, USA

<sup>2</sup>Earth Systems Observations, Los Alamos National Lab, Los Alamos, NM, USA

<sup>3</sup>Department of Materials Science and Engineering, University of Illinois at Urbana-Champaign, Urbana, IL, USA

Correspondence to: D. J. Wuebbles (wuebbles@atmos.uiuc.edu)

Received: 16 March 2012 – Published in Atmos. Chem. Phys. Discuss.: 6 August 2012

Revised: 14 May 2013 – Accepted: 23 May 2013 – Published: 1 July 2013

**Abstract.** The prospective future adoption of molecular hydrogen (H<sub>2</sub>) to power the road transportation sector could greatly improve tropospheric air quality but also raises the question of whether the adoption would have adverse effects on the stratospheric ozone. The possibility of undesirable impacts must be fully evaluated to guide future policy decisions. Here we evaluate the possible impact of a future (2050) H<sub>2</sub>-based road transportation sector on stratospheric composition and chemistry, especially on the stratospheric ozone, with the MOZART (Model for OZone And Related chemical Tracers) model. Since future growth is highly uncertain, we evaluate the impact of two world evolution scenarios, one based on an IPCC (Intergovernmental Panel on Climate Change) high-emitting scenario (A1FI) and the other on an IPCC low-emitting scenario (B1), as well as two technological options: H<sub>2</sub> fuel cells and H<sub>2</sub> internal combustion engines. We assume a H<sub>2</sub> leakage rate of 2.5 % and a complete market penetration of H<sub>2</sub> vehicles in 2050. The model simulations show that a H<sub>2</sub>-based road transportation sector would reduce stratospheric ozone concentrations as a result of perturbed catalytic ozone destruction cycles. The magnitude of the impact depends on which growth scenario evolves and which H<sub>2</sub> technology option is applied. For the evolution growth scenario, stratospheric ozone decreases more in the H<sub>2</sub> fuel cell scenarios than in the H<sub>2</sub> internal combustion engine scenarios because of the NO<sub>x</sub> emissions in the latter case. If the same technological option is applied, the impact is larger in the A1FI emission scenario. The largest impact, a 0.54 % decrease in annual average global mean

stratospheric column ozone, is found with a H<sub>2</sub> fuel cell type road transportation sector in the A1FI scenario; whereas the smallest impact, a 0.04 % increase in stratospheric ozone, is found with applications of H<sub>2</sub> internal combustion engine vehicles in the B1 scenario. The impacts of the other two scenarios fall between the above two boundary scenarios. However, the magnitude of these changes is much smaller than the increases in 2050 stratospheric ozone projected, as stratospheric ozone is expected to recover due to the limits in ozone depleting substance emissions imposed in the Montreal Protocol.

## 1 Introduction

Molecular hydrogen (H<sub>2</sub>) is being considered as a key energy carrier for transportation systems of the future because it is potentially cleaner and more efficient than fossil fuels. The large-scale adoption of H<sub>2</sub> to replace fossil fuel in the road transportation sector would change the composition of the atmosphere through changes in the emissions of several important chemical species. Atmospheric H<sub>2</sub> concentrations would likely increase due to leakage during its production, transportation and storage processes while emissions of fossil fuel combustion byproducts, including nitrogen oxides (NO<sub>x</sub> = NO + NO<sub>2</sub>), carbon monoxide (CO) and volatile organic compounds (VOCs), would likely decrease.

There have been a number of studies on the possible impacts of such a transition on stratospheric composition

and chemistry due to concerns that significant reductions in stratospheric ozone from a H<sub>2</sub> economy would lead to increased UV radiation reaching the earth's surface. However, no consensus has been achieved on how stratospheric ozone would change as a result of application of H<sub>2</sub> technologies. Under a somewhat extreme assumption of more than quadrupled surface H<sub>2</sub> concentration (2.3 ppmv), and with no changes in fossil fuel combustion related emissions, a 2-D coupled chemistry-climate model study by Tromp et al. (2003) found spatial and temporal enhancement of polar ozone holes, leading to ozone depletion of 3–8 %, due to lowered stratospheric temperatures, a result of increased stratospheric water vapor from oxidized H<sub>2</sub>. Warwick et al. (2004) found a slight increase (0.1–0.6 %) in stratospheric ozone, considering associated changes in CO, NO<sub>x</sub>, VOCs emissions with H<sub>2</sub> fuel cells in a 2-D chemistry transport model, with an assumed H<sub>2</sub> leakage rate of 5 %. Based on a coupled chemistry-climate model study, Jacobson (2008) reported a 0.41 % increase in global column ozone, assuming H<sub>2</sub> fuel cell vehicles with their associated decrease in fossil fuel combustion related emissions and a 3.2 % decrease in atmospheric H<sub>2</sub> concentrations due to a 3 % leakage rate.

In these previous studies the transition to H<sub>2</sub> technology was assumed to take place immediately with the then current (ca. 2000) background atmosphere. In the real world, however, this transition will take some time to occur, because the industry of H<sub>2</sub> production and the infrastructure of H<sub>2</sub> delivery are not ready, and several technological barriers need yet to be tackled. Considering these factors, we assume a gradual rather than an abrupt transition to a H<sub>2</sub> powered road transportation sector, with an assumed completion by 2050. That is, all on-road vehicles operating in 2050 will be powered by H<sub>2</sub>. This is particularly relevant to evaluating the stratospheric impacts since the composition of the background atmosphere in 2050 is expected to be different than the current atmosphere, especially with regards to the decline of CFCs and other ozone depleting substances due to the implementation of the Montreal Protocol.

We investigate potential changes in catalytic cycles that determine stratospheric ozone concentrations in response to the adoption of a H<sub>2</sub>-based road transportation sector, assuming a perhaps more realistic H<sub>2</sub> leakage rate of 2.5 % (Schultz et al., 2003; Warwick et al., 2004). Given the uncertainties in projections of future growth and emissions, we evaluate emissions scenarios that encompass several possible growth and technology adoption paths. The growth scenarios are based on the high and low emitting Intergovernmental Panel on Climate Change (IPCC) Special Report on Emissions Scenarios (SRES), A1FI and B1, respectively. The technological adoption scenarios include H<sub>2</sub> fuel cell and H<sub>2</sub> internal combustion engine options. The impacts of these emissions are evaluated using the Model for OZone and Related chemical Tracers version 3.1 (MOZART 3.1) three-dimensional chemistry transport model. This is the second paper of two papers on the impacts of a H<sub>2</sub>-based road trans-

portation sector with emphasis on the stratospheric ozone, the first focused on tropospheric chemistry (Wang et al., 2013).

## 2 Emission scenarios

Here we carry out model simulations along with the highest and lowest Intergovernmental Panel on Climate Change (IPCC) Special Report on Emissions Scenarios (SRES) (IPCC, 2000), A1FI and B1, respectively. For each of these two IPCC scenarios, a baseline and two H<sub>2</sub> scenarios are further assumed. (1) The baseline (BL) scenario is the reference scenario for 2050 in which fossil fuel powered vehicles are still the dominant mode of transportation. (2) In the H<sub>2</sub> fuel cell (H<sub>2</sub>-FC) scenario, energy demands of the road transportation sector are met by H<sub>2</sub> fuel cell technology; H<sub>2</sub> emissions due to leakage as well as reductions in combustion-related emissions of H<sub>2</sub>, NO<sub>x</sub>, VOCs, CO and SO<sub>2</sub> are included. (3) In the H<sub>2</sub> internal combustion engine (H<sub>2</sub>-ICE) scenario, energy demands of the road transportation sector are met by H<sub>2</sub> using internal combustion technology. In this scenario, H<sub>2</sub> emissions due to leakage as well as reductions in combustion-related emissions of H<sub>2</sub>, VOCs, CO and SO<sub>2</sub> are included, as in H<sub>2</sub>-FC; however, unlike H<sub>2</sub>-FC scenario, there are no reductions in NO<sub>x</sub> emissions because NO<sub>x</sub> is still a byproduct of internal combustion process regardless of the type of fuel.

The future emissions of H<sub>2</sub>, NO<sub>x</sub>, CO, and several NMVOCs (non-methane VOCs) in these assumed scenarios are the same as described in Wang et al. (2013), with the exception of aerosol emissions, which are not included in MOZART 3.1; we assume a H<sub>2</sub>:CO mass emission factor of 0.03 for fossil fuel combustion and a H<sub>2</sub> leakage rate of 2.5 %. For more details see Wang et al. (2013). A short description of related emissions is presented here.

Annual global emissions of H<sub>2</sub>, CO, NMVOCs and NO<sub>x</sub> of current (2000) and 2050 (baseline and H<sub>2</sub> scenarios) are listed in Table 1. Global emissions increase relative to 2000 in the 2050 A1FI baseline (A1FI BL) scenario for H<sub>2</sub> (42 %), CO (35 %), NMVOCs (28 %) and NO<sub>x</sub> (115 %). In the 2050 B1 baseline (B1 BL) scenario, global emissions decrease from 2000 for H<sub>2</sub> (19 %), CO (10 %) and NMVOCs (6 %); NO<sub>x</sub> emissions increase by 5 %.

In the A1FI scenarios with a H<sub>2</sub> road transportation sector, global H<sub>2</sub> emissions increase by 81 % relative to the 2050 A1FI baseline (A1FI BL) scenario, or increase by 157 % from the 2000 emissions. Meanwhile, global emissions in the 2050 H<sub>2</sub>-FC and H<sub>2</sub>-ICE scenarios decrease for CO (25 %), NMVOCs (14 %) and NO<sub>x</sub> (29 % in H<sub>2</sub>-FC; 0 % in H<sub>2</sub>-ICE), compared to the 2050 A1FI baseline (A1FI BL) scenario. If compared with the 2000 emissions, in a 2050 A1FI world with a H<sub>2</sub> road transportation sector, emissions increase to a lesser extent than in the A1FI baseline scenario: CO (1.6 %), NMVOCs (10 %) and NO<sub>x</sub> (53 % in H<sub>2</sub>-FC).

**Table 1.** Annual mean global emissions of key species for the scenarios developed for this study.

| Species                       | H <sub>2</sub>      | CO                  | NO <sub>x</sub>      | NMVOCS              |
|-------------------------------|---------------------|---------------------|----------------------|---------------------|
| Unit                          | Tg yr <sup>-1</sup> | Tg yr <sup>-1</sup> | TgN yr <sup>-1</sup> | Tg yr <sup>-1</sup> |
| 2000                          | 40.0                | 1361.2              | 43.8                 | 469.6               |
| 2050 A1FI BL                  | 56.6                | 1844.7              | 94.3                 | 600.9               |
| 2050 A1FI H <sub>2</sub> -FC  | 102.7               | 1383.4              | 67.2                 | 518.5               |
| 2050 A1FI H <sub>2</sub> -ICE | 102.7               | 1383.4              | 94.3                 | 518.5               |
| 2050 B1 BL                    | 32.4                | 1223.3              | 46.0                 | 442.7               |
| 2050 B1 H <sub>2</sub> -FC    | 53.2                | 1107.1              | 34.8                 | 408.5               |
| 2050 B1 H <sub>2</sub> -ICE   | 53.2                | 1107.1              | 46.0                 | 408.5               |

In the B1 scenarios with a H<sub>2</sub> road transportation sector, global H<sub>2</sub> emissions increase by 64 % relative to the 2050 B1 baseline (B1 BL) scenario, or increase by 33 % from the 2000 emissions. Concurrently, global emissions in the 2050 H<sub>2</sub>-FC and H<sub>2</sub>-ICE scenarios decrease for CO (10 %), NMVOCS (8 %) and NO<sub>x</sub> (24 % in H<sub>2</sub>-FC; 0 % in H<sub>2</sub>-ICE), compared to the 2050 B1 baseline (B1 BL) scenario. If compared with the 2000 emissions, in a 2050 B1 world with a H<sub>2</sub> road transportation sector, emissions decrease to a greater extent than in the B1 baseline scenario: CO (19 %), NMVOCS (13 %) and NO<sub>x</sub> (20 % in H<sub>2</sub>-FC).

These emissions are input to the model as monthly varying maps at the model resolution.

### 3 Model description

In this study, we evaluate the atmospheric impacts with the Model for OZone And Related chemical Tracers (MOZART) version 3.1 global chemistry transport model. MOZART-3 has been used and evaluated in a number of studies (e.g., Gettelman et al., 2004; Kinnison et al., 2007; Kulawik et al., 2006; Liu et al., 2009, 2011; Pan et al., 2007; Park et al., 2004). The model simulates the atmosphere from the surface to 0.001 Pa level (~115 km) by dividing it vertically into 60 layers. Horizontally the globe is partitioned into 96 grids on latitude and 144 grids on longitude, corresponding to a resolution of 1.9° × 2.5° (latitude × longitude). It simulates in a detailed fashion the physical and chemical processes of the troposphere and stratosphere. It has 108 species, 71 photochemical reactions, 218 gas phase reactions and 18 heterogeneous reactions, including heterogeneous chemistry in the stratosphere and polar stratospheric cloud processes. The model is driven with meteorology from a year of simulation of the Whole-Atmosphere Community Climate Model version 3 (WACCM-3) (Sassi et al., 2005), which represents the mid-1990s atmosphere. This meteorology is repeated for each year for multiyear simulations. We have chosen to use this meteorology since in this study we focus on emissions changes' impacts on photochemistry and because predicting meteorological conditions in 2050 with reasonable confidence is highly difficult. In addition, previous studies (e.g.,

Lin et al., 2008; Wu et al., 2008) have shown that emissions changes will likely be more important than changes in climate on atmospheric composition and chemistry in the future.

The model is integrated with a time step of 15 min. After completion of one year's calculations, the meteorology field is repeated for the next year. This method allows the impact of changes in emissions to be investigated, excluding the possible influences of changes in meteorology. The lower boundary concentrations of CH<sub>4</sub> and N<sub>2</sub>O are set to 2.4 ppmv and 0.35 ppmv, respectively, according to the IPCC A1B scenario (IPCC, 2000). Lower boundary conditions for halocarbons are prescribed according to the 2050 concentrations in the Ab baseline scenario developed by the World Meteorological Organization (WMO, 2003). The model is run for 12 yr and has reached steady state. Our analysis is based on results from the last year of simulation.

## 4 Model results and discussion

In this section we describe and discuss the results of the model simulations. Here, the stratosphere refers to the model levels above the tropopause and we adopt the World Meteorological Organization (WMO) definition of tropopause, i.e., the lowest level at which the lapse rate decreases to 2 K km<sup>-1</sup> or less. Our modeling results show that the combined effect of increased H<sub>2</sub> emissions and other emission changes in a H<sub>2</sub>-based road transport sector would tend to decrease ozone concentrations in the stratosphere in all scenarios except for the B1 H<sub>2</sub>-ICE scenario. The overall effects on annually, globally averaged stratospheric column ozone are -0.54 %, -0.23 %, -0.20 % and +0.04 % for A1FI H<sub>2</sub>-FC, A1FI H<sub>2</sub>-ICE, B1 H<sub>2</sub>-FC and B1 H<sub>2</sub>-ICE scenarios, respectively. First we will analyze the baseline scenarios with a fossil fuel based road transportation sector and then the scenarios with H<sub>2</sub> technologies will be discussed and compared with the baseline scenario.

### 4.1 Baseline scenarios

In the 2050 baseline simulations, stratospheric ozone has recovered to a significant extent compared with today's atmosphere, as would be expected from future decline of atmospheric halogen concentrations. On an annual mean global average basis, stratospheric column ozone increases from the mid-1990s atmosphere by ~13 DU (1 Dobson unit (DU) corresponds to 2.69 × 10<sup>20</sup> ozone molecules per square meter) in the 2050 A1FI BL scenario and by ~11 DU in the 2050 B1 BL scenario. Figure 1 shows stratospheric column ozone and its increase from the current atmosphere as a function of latitude and time of year in the two baseline scenarios. The increase is not uniform in space and time. The increase rate is the lowest in the tropics, where stratospheric ozone increases by ~5 DU. Outside the tropics, the increase is generally

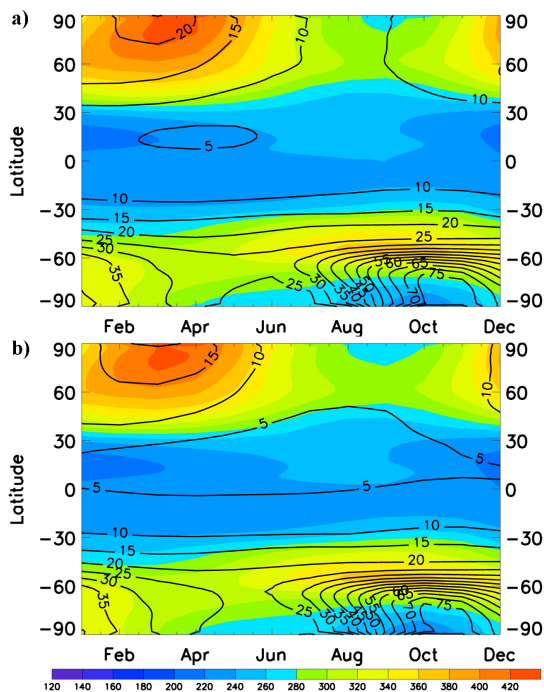


**Fig. 1.** 2050 zonal mean stratospheric column O<sub>3</sub> (shown by color in units of DU) and the increase from today's atmosphere (a model run representing mid-1990s atmosphere) (shown by contours in units of DU) as a function of latitude and time of a year for (a) A1FI BL and (b) B1 BL scenarios.

greater than in the tropics, but bears inter-hemispheric asymmetry; the increase in the Southern Hemisphere is generally greater than in the Northern Hemisphere. The increase in the hemispheric spring is largest throughout a year. Arctic stratospheric column ozone increases by  $\sim 20$  and  $\sim 15$  DU in the 2050 A1FI and B1 baseline scenarios. In October and November Antarctic stratospheric column ozone increases by more than 70 DU from the current value ( $\sim 150$  DU) to  $\sim 220$  DU, signaling a partial but still significant Antarctic ozone hole recovery. These results are within the range reported in WMO (2011). The recovery of the Antarctica ozone hole in October compares well with the average of model simulations in WMO (2011).

#### 4.2 H<sub>2</sub> fuel cell scenarios

The annual mean global average stratospheric column ozone in the A1FI H<sub>2</sub>-FC scenario decreases by 0.54 % ( $\sim 1.5$  DU) from the A1FI baseline. In the tropics, zonal mean stratospheric column ozone decreases by less than 1 DU from December to May; whereas it decreases by 1–1.5 DU from June to November (Fig. 2a). Outside the tropics, the reductions are even larger (greater than 1.5 DU). There is a large decrease (more than 2 DU) occurring north of 35° N from September to February, with the maximum reduction of 2.5 DU (0.8 %) appearing at  $\sim 40^\circ$  N in October. There is also a more than

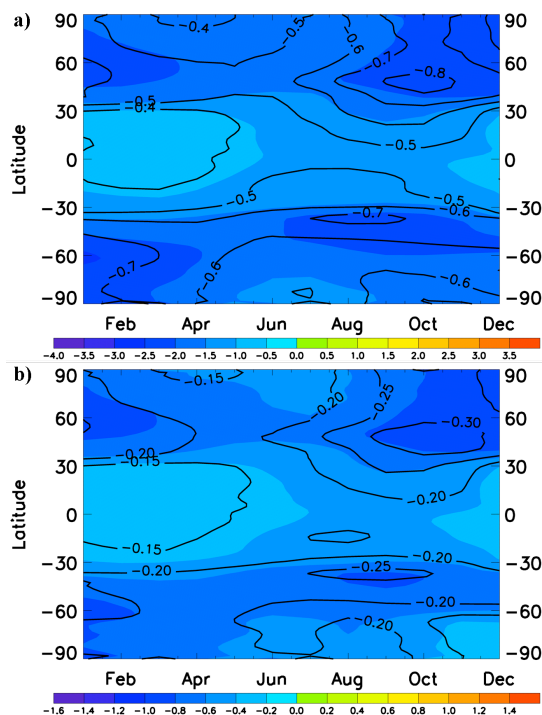


**Fig. 2.** Zonal mean stratospheric column O<sub>3</sub> changes in units of DU (shown by color) and the relative change in % (shown by contours) in the H<sub>2</sub>-FC scenarios compared with the BL scenarios as a function of latitude and time of a year for (a) A1FI and (b) B1 scenarios.

2 DU reduction in the southern mid-latitudes from mid-June to March.

In the B1 H<sub>2</sub>-FC scenario the annual, global mean stratospheric column ozone decreases by 0.20 % ( $\sim 0.5$  DU) from the B1 baseline scenario. The pattern of decrease is similar to that in the A1FI scenario, but the magnitude is smaller (Fig. 2b). The decrease in the tropics does not exceed 0.6 DU (or 0.2 %) throughout a year, while the decrease is even smaller ( $< 0.4$  DU or 0.15 %) from December to June. Again, there are larger reductions outside the tropics (greater than 0.6 DU or 0.2 %). In the Northern Hemisphere, there is a significant decrease (more than 0.8 DU) present north of 35° N from September to February. In the SH, there is a band of significant decrease (more than 0.6 DU or 0.2 %) between 30° S and 60° S.

In both the A1FI and B1 H<sub>2</sub>-FC scenarios, ozone concentrations are reduced throughout most of the stratosphere; however, there is a layer of slight increase of less than 1 %, or  $1 \times 10^{10}$  molecules cm<sup>-3</sup>, in the middle stratosphere (Fig. 3). This layer of increased ozone is about 10 km thick and starts from  $\sim 20$  km altitude in the poles and from  $\sim 29$  km altitude in the tropics. Above this layer in the upper stratosphere, ozone concentrations are reduced by less than  $1 \times 10^{10}$  molecules cm<sup>-3</sup>, or 1 %. Below the increased ozone layer, the ozone concentration reductions are greater as the altitude decreases.



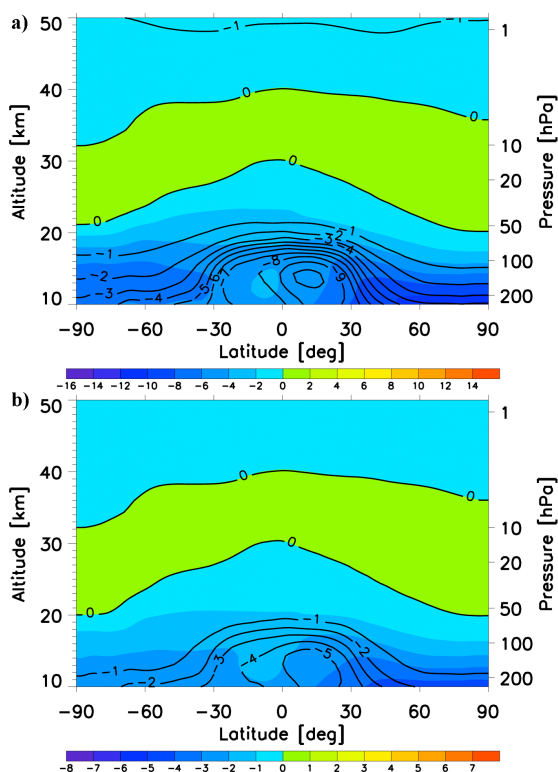


**Fig. 3.** Annually, zonally averaged O<sub>3</sub> concentration changes in units of 10<sup>10</sup> molecules cm<sup>-3</sup> (shown by color) and the relative change in % (shown by contours) in the H<sub>2</sub>-FC scenarios compared with the BL scenarios as a function of latitude and altitude for (a) A1FI and (b) B1 scenarios.

The most significant reductions in annual, zonal mean ozone concentrations are in the upper troposphere/lower stratosphere (UT/LS) region. At each altitude level, ozone concentrations decreased more near the poles (up to  $10 \times 10^{10}$  molecules cm<sup>-3</sup> in A1FI and up to  $5 \times 10^{10}$  molecules cm<sup>-3</sup> in B1) than in the tropics (around  $4 \times 10^{10}$  molecules cm<sup>-3</sup> in A1FI and around  $2 \times 10^{10}$  molecules cm<sup>-3</sup> in B1). The relative reduction, however, is greater in the tropics as there is less ozone in the baseline scenario. The maximum zonal mean O<sub>3</sub> relative reduction (up to 10 % in A1FI and up to 5 % in B1) is at approximately 13 km altitude around 15° N. In the lowermost stratosphere, ozone reductions occur partly because of the influence of the underlying troposphere, where ozone concentrations are reduced due to the reduced tropospheric ozone precursor emissions associated with the adoption of H<sub>2</sub> fuel cells (Wang et al., 2013), and partly because local ozone production is reduced as a result of a strong reduction in NO<sub>x</sub> concentrations. As shown in Fig. 4, NO<sub>x</sub> mixing ratios in the tropical UT/LS region decrease by up to 12 % (75 pptv) in the A1FI and by up to 8 % (30 pptv) in the B1 H<sub>2</sub>-FC scenarios relative to their corresponding baseline scenarios. The reduction in the tropical ozone production reduces

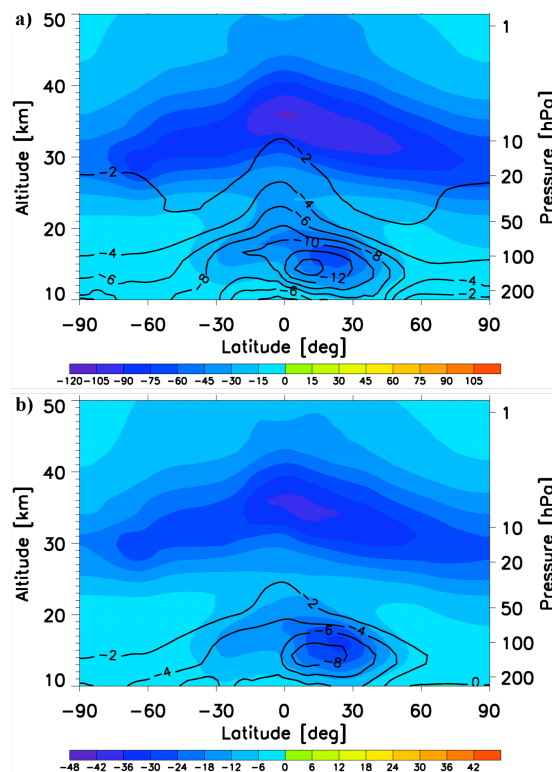


**Fig. 4.** Annually, zonally averaged NO<sub>x</sub> concentration changes in units of pptv (shown by color) and the relative change in % (shown by contours) in the H<sub>2</sub>-FC scenarios compared with the BL scenarios as a function of latitude and altitude for (a) A1FI and (b) B1 scenarios.

the amount of ozone transported to the mid-latitudes and the poles. The impact of the tropospheric air and the tropospheric ozone formation mechanism on UT/LS ozone concentrations diminishes with increasing altitude. At higher altitudes, perturbations to the catalytic ozone destruction cycles contribute more to the changes in ozone concentrations.

The effects on O<sub>3</sub> discussed so far have focused on changes in O<sub>3</sub> due to changes in emissions associated with a conversion to a hydrogen powered road transportation sector. However, changes in CH<sub>4</sub>, which was implemented as a lower boundary condition in these simulations, also affects stratospheric ozone. Based on simulations of changes in O<sub>3</sub> due to changes in the CH<sub>4</sub> boundary condition, we estimate the sensitivity of stratospheric ozone to be 0.5 % per ppm CH<sub>4</sub> change. The total ozone sensitivity for this simulation was 1.8 % per ppm CH<sub>4</sub>, which is in agreement with other studies (e.g., Wuebbles and Hayhoe, 2000; Fleming et al., 2011). Using the calculated sensitivity and estimated changes in CH<sub>4</sub> from changes in the CH<sub>4</sub> lifetime in the perturbed simulations (e.g., Fugelstvedt et al., 1999), we estimate that changes in stratospheric O<sub>3</sub> due to changes in CH<sub>4</sub> would be +0.1 % for the A1FI scenario and +0.08 % for the

B1 scenario, with the largest changes occurring in the lower stratosphere.

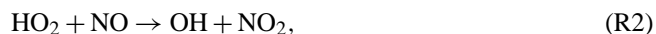
In the mid-latitude lower stratosphere, it is well established that catalytic cycles involving HO<sub>x</sub> dominate local ozone destruction (e.g., Wennberg et al., 1994; WMO, 1995). In these model simulations, HO<sub>x</sub> catalytic cycles contribute the most to the ozone loss rate in the stratosphere below 20 km altitude at 35° N at the September equinox. HO<sub>x</sub> concentrations are predicted to increase by around 3 % ( $\sim 1 \times 10^5$  molecules cm<sup>-3</sup>) and 1 % ( $\sim 0.5 \times 10^5$  molecules cm<sup>-3</sup>) for the A1FI and B1 scenarios, respectively (Fig. 5). These increases in the stratosphere are largely due to increases in H<sub>2</sub> concentrations and oxidation. As a direct result, the ozone loss cycles catalyzed by HO<sub>x</sub> are enhanced.

At the same time, NO<sub>x</sub> concentrations are reduced throughout the stratosphere in the H<sub>2</sub>-FC scenarios (Fig. 4). The increased stratospheric HO<sub>x</sub> concentrations contribute to the reductions in stratospheric NO<sub>x</sub> through the reaction



Additionally, stratospheric NO<sub>x</sub> is also likely to be affected by the drastic changes in tropospheric NO<sub>x</sub> concentration in the H<sub>2</sub>-FC scenarios. The major source of NO<sub>x</sub> in the stratosphere is the reaction of N<sub>2</sub>O with O(<sup>1</sup>D). However, N<sub>2</sub>O and O(<sup>1</sup>D) concentrations are not significantly affected by the perturbation of a H<sub>2</sub>-FC sector. It has been proposed that reactive nitrogen (NO<sub>y</sub>) in the upper troposphere over tropical regions can significantly impact lower stratosphere NO<sub>y</sub> concentrations (Ko et al., 1986) due to NO<sub>y</sub>'s longer lifetime than NO<sub>x</sub> and strong upwelling in this region. This hypothesis is supported by observations (e.g., Murphy et al., 1993). In this study, NO<sub>y</sub> concentrations in the UT/LS region in 2050 are calculated to be about 1 ppbv in all scenarios, exceeding the threshold mixing ratio of 0.6 ppbv suggested by Murphy et al. (1993). Therefore, increased NO<sub>y</sub> concentrations in the UT/LS region are likely to impact the stratospheric NO<sub>y</sub> abundance. In the H<sub>2</sub>-FC scenarios, model results show that NO<sub>y</sub> concentrations in the UT/LS region are significantly reduced (by  $\sim 15$  % for A1FI and by  $\sim 8$  % for B1), likely leading to decreased NO<sub>x</sub> and NO<sub>y</sub> in the stratosphere.

Furthermore, the NO<sub>x</sub> reduction impacts the HO<sub>x</sub> cycles through Reaction (R1) and



hence affecting HO<sub>x</sub> as well as the partitioning between HO<sub>2</sub> and OH. In this case, HO<sub>2</sub> concentrations increase due to decreased availability of NO in Reaction (R2), leading to enhanced ozone loss since the rate of HO<sub>x</sub> cycles is dependent on HO<sub>2</sub> concentrations to the first order. Meanwhile, the rate of Reaction (R1) would fall as NO concentrations decrease, making Reaction (R1) a smaller HO<sub>x</sub> sink.

Both of these effects tend to further enhance the HO<sub>x</sub> cycles. As shown in Fig. 6, the daily average ozone destruction

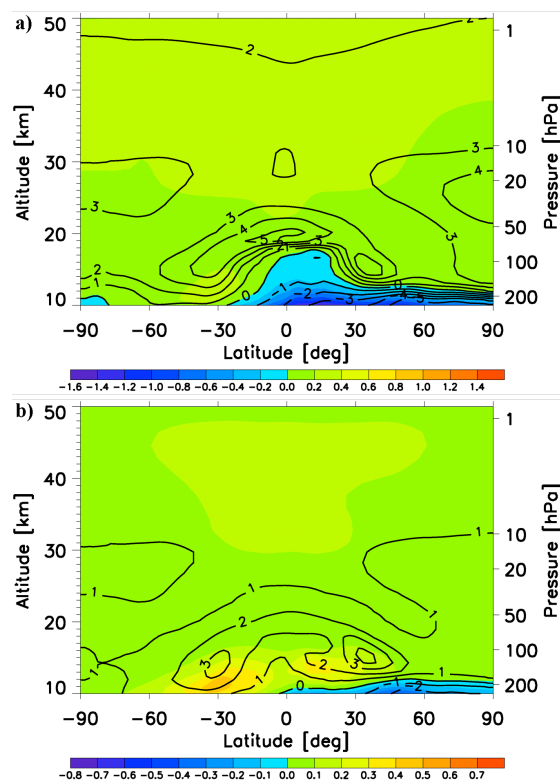


**Fig. 5.** Annually, zonally averaged HO<sub>x</sub> concentration changes in units of  $10^6$  molecules cm<sup>-3</sup> (shown by color) and the relative change in % (shown by contours) in the H<sub>2</sub>-FC scenarios compared with the BL scenarios as a function of latitude and altitude for (a) A1FI and (b) B1 scenarios.

rate by the HO<sub>x</sub> cycles at 35° N at the September equinox increases by 2 % (A1FI) and 1 % (B1) at 20 km altitude (Fig. 6); the total ozone destruction rate by all catalytic cycles increases by 0.5 % (A1FI) and 0.2 % (B1) due to enhanced HO<sub>x</sub> cycles.

In addition to promoting the HO<sub>x</sub> cycles, a decrease in NO<sub>x</sub> concentrations also leads to an enhancement of the halogen cycles via NO<sub>x</sub>/halogen cycles coupling. Nevertheless, this enhancement would have a smaller impact on ozone concentrations since in 2050, halogen cycles are only responsible for a few percent of ozone destruction rate in the lower stratosphere, in which stratospheric halogen loading is expected to be significantly smaller than today's. As shown in Fig. 6, the overall ozone destruction rate is enhanced by 0.1 % in the A1FI and 0.04 % in the B1 scenarios due to the halogen cycles at 35° N at the September equinox at 20 km level. In sum, the decrease in ozone concentrations in the lower stratosphere in the A1FI and B1 H<sub>2</sub>-FC scenarios is primarily due to an intensification of the HO<sub>x</sub> catalyzed O<sub>3</sub> destruction cycles.

In the middle stratosphere (25–35 km altitude in the tropics, somewhat lower at higher latitudes), annually, zonally averaged ozone concentrations increase by up to 0.4 % in

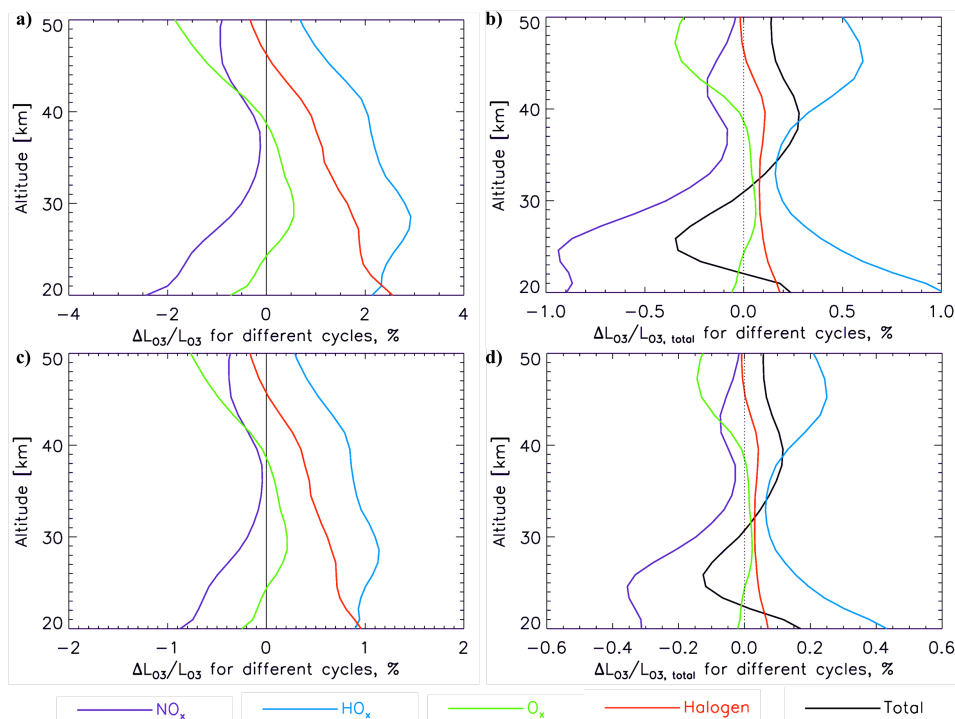


**Fig. 6.** Changes in contributions of different catalytic O<sub>3</sub> destruction cycles to the total O<sub>3</sub> loss in the H<sub>2</sub>-FC scenarios compared to the baseline scenario. Panels (a) and (b) are for A1FI and panels (c) and (d) are for B1. (a) and (c) % change in contribution of each catalytic cycle compared to its contribution in the BL; (b) and (d) % change in contributions of different catalytic O<sub>3</sub> destruction cycles compared to the total O<sub>3</sub> loss rate in BL. All figures are daily averaged values for the September equinox at 35° N.

both the A1FI and B1 H<sub>2</sub>-FC scenarios (Fig. 3). Even though ozone loss rate due to HO<sub>x</sub> catalytic cycles increases due to the previously discussed mechanisms in this region, the overall ozone loss rate is slowed down because NO<sub>x</sub> cycles dominate ozone loss in the middle stratosphere and NO<sub>x</sub> concentrations are reduced in this region. As shown in Fig. 4, annually, zonally averaged NO<sub>x</sub> concentrations decrease by ~ 3 % (~ 50 pptv) in the A1FI and by ~ 2 % (~ 20 pptv) in the B1 scenario. The NO<sub>x</sub> concentration decrease is due to enhancement of Reaction (R1), through which increased HO<sub>x</sub> concentrations make this reaction a larger NO<sub>x</sub> sink, likely due to decreases in NO<sub>x</sub> concentrations in the underlying atmosphere. The ozone loss rate due to NO<sub>x</sub> catalyzed cycles is reduced throughout most of the stratosphere (Fig. 6); however, its impact on ozone concentrations is only significant in the middle stratosphere where NO<sub>x</sub> cycles dominate ozone destruction. As shown in Fig. 6, the overall ozone destruction rate at 25 km altitude at 35° N at the September equinox is decreased by 0.35 % in the A1FI scenario and by 0.13 % in the B1 scenario due to the attenuation of the NO<sub>x</sub> catalyzed ozone destruction cycles. Therefore, a slight ozone concentration increase is calculated in the middle stratosphere in both the H<sub>2</sub>-FC scenarios. The increase in ozone concentration in the middle stratosphere, however, cannot fully com-

pensate for the decrease in the lower stratosphere since ozone molecules per unit volume is lower at higher altitude.

In the upper stratosphere, HO<sub>x</sub> catalyzed cycles again dominate ozone loss cycles. The HO<sub>x</sub> concentrations increase by 2–3 % in the A1FI and by ~ 1 % in the B1 scenarios (Fig. 5). This increase is due to enhanced H<sub>2</sub> abundance and the decline in the rate of Reaction (R1) as a result of the NO<sub>x</sub> concentrations decrease. As a direct result, HO<sub>x</sub> catalyzed cycles are enhanced. As shown in Fig. 6, the ozone destruction rate due to HO<sub>x</sub> cycles at 25 km altitude at 35° N at the September equinox level is increased by 0.3 % in the A1FI and 0.13 % in the B1 scenarios. The resulting O<sub>3</sub> concentration decline in this region is less than 1 % in the A1FI and B1 H<sub>2</sub>-FC scenarios (Fig. 3). Its impact on stratospheric column ozone is small, owing to the low molecule concentrations at such high altitudes.

#### 4.3 H<sub>2</sub> internal combustion engine scenarios

The overall impact of a H<sub>2</sub>-ICE road transportation sector on stratospheric ozone concentration is smaller compared with the corresponding H<sub>2</sub>-FC scenarios, mainly because of NO<sub>x</sub> being higher for the ICE scenarios. The annually, globally averaged stratospheric column ozone in the A1FI H<sub>2</sub>-ICE scenario would be reduced by 0.23 %, or 0.5 DU. Stratospheric

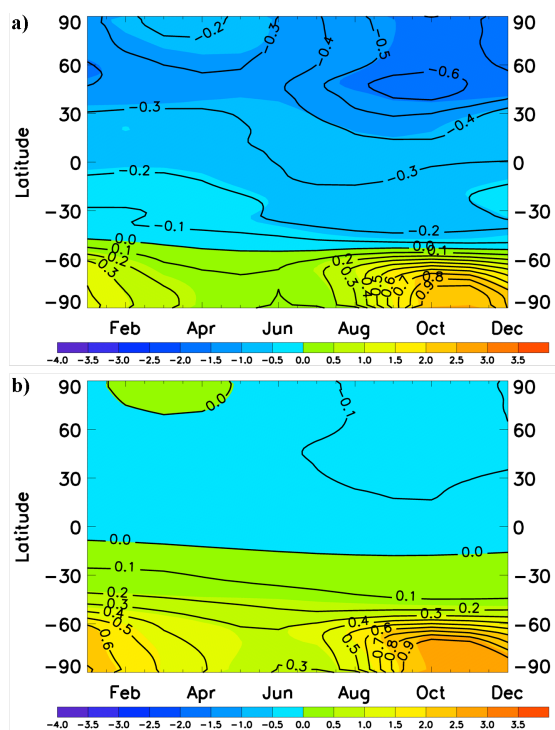


**Fig. 7.** Zonal mean stratospheric column O<sub>3</sub> changes in units of DU (shown by color) and the relative change in % (shown by contours) in the H<sub>2</sub>-ICE scenarios compared with the BL scenarios as a function of latitude and time of a year for (a) A1FI and (b) B1 scenarios.

column ozone decreases north of 50° S but increases south of this latitude (Fig. 7a). In the tropics, stratospheric column ozone decreases by 0.1–0.3 %, or 0–1 DU throughout a year. In the northern mid- and high-latitudes, stratospheric column ozone decreases by more than 1 DU. The greatest decrease (1.5 DU or 0.6 %) occurs at the northern mid-latitudes from September to January. In the Antarctic region, stratospheric column ozone increases by up to 3 DU, or 1 % from October to December.

From the zonal average perspective, annual mean ozone concentrations are reduced in the lower stratosphere in the A1FI H<sub>2</sub>-ICE scenario (Fig. 8a). In the tropics, the reduction extends to the middle stratosphere (30 km altitude). The maximum relative reduction (5 %) occurs at 17 km altitude just north of the Equator, whereas the largest concentration change (a decrease of  $8 \times 10^{10}$  molecules cm<sup>-3</sup>) is at 12 km in the Arctic region. There are very slight ozone reductions above 45 km altitude in the tropics and above 48 km altitude in the poles. Ozone concentrations are increased in the rest of the stratosphere, but the relative increase does not exceed 1 %. There is an increase of up to  $8 \times 10^{10}$  molecules cm<sup>-3</sup> around 18 km in the Antarctic region. Changes in stratospheric O<sub>3</sub> due to decreases in CH<sub>4</sub> are estimated to be –0.08 % for the A1FI scenario and –0.03 % for the B1 scenario.

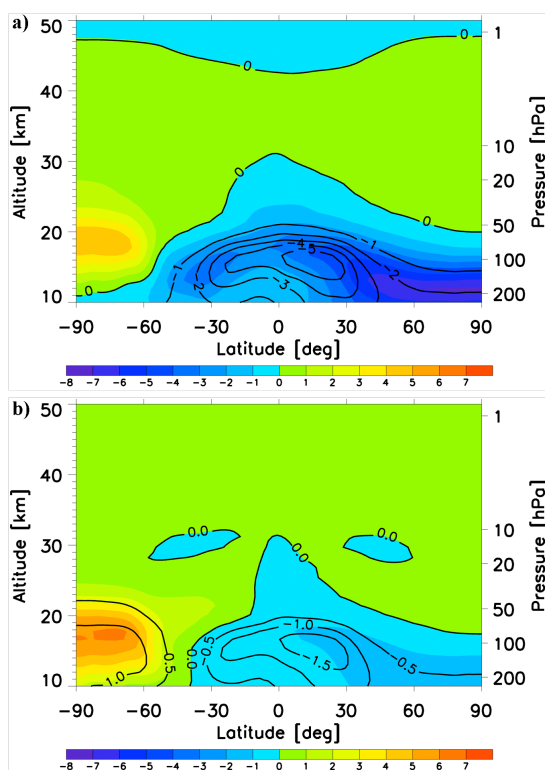


**Fig. 8.** Annually, zonally averaged O<sub>3</sub> concentration changes in units of  $10^{10}$  molecules cm<sup>-3</sup> (shown by color) and the relative change in % (shown by contours) in the H<sub>2</sub>-ICE scenarios compared with the BL scenarios as a function of latitude and altitude for (a) A1FI and (b) B1 scenarios.

As in the H<sub>2</sub>-FC scenarios, ozone concentration changes in the H<sub>2</sub>-ICE scenarios are a result of changes in radical concentrations, which affect the catalytic cycles destructing stratospheric ozone. HO<sub>x</sub> concentrations decrease in the upper troposphere due to the reduced NMVOCs emissions in the A1FI H<sub>2</sub>-ICE scenario, as NMVOCs oxidation provides a HO<sub>x</sub> source in the upper troposphere. Increased NO<sub>x</sub> concentrations (Fig. 10a) also contribute to the HO<sub>x</sub> decrease through Reaction (R1). This decrease penetrates into the lower stratosphere with rising air from the tropics, and overcomes the increase in HO<sub>x</sub> due to increased H<sub>2</sub> oxidation. Figure 9a shows the pattern of HO<sub>x</sub> reductions, which diminish with altitude. Above 20 km in the tropics and above 15 km near the poles, HO<sub>x</sub> concentrations increase slightly as the H<sub>2</sub> leaked into the atmosphere provides a HO<sub>x</sub> source in the stratosphere.

NO<sub>x</sub> concentrations decrease in the middle stratosphere but increase in the upper and lower stratosphere in the A1FI H<sub>2</sub>-ICE scenario (Fig. 10a). In the lower stratosphere NO<sub>x</sub> concentrations increase because of the NO<sub>x</sub> budget increase throughout the troposphere since, in the H<sub>2</sub>-ICE scenarios, NO<sub>x</sub> is still emitted as combustion byproduct of internal combustion engines (Wang et al., 2013). Meanwhile, the



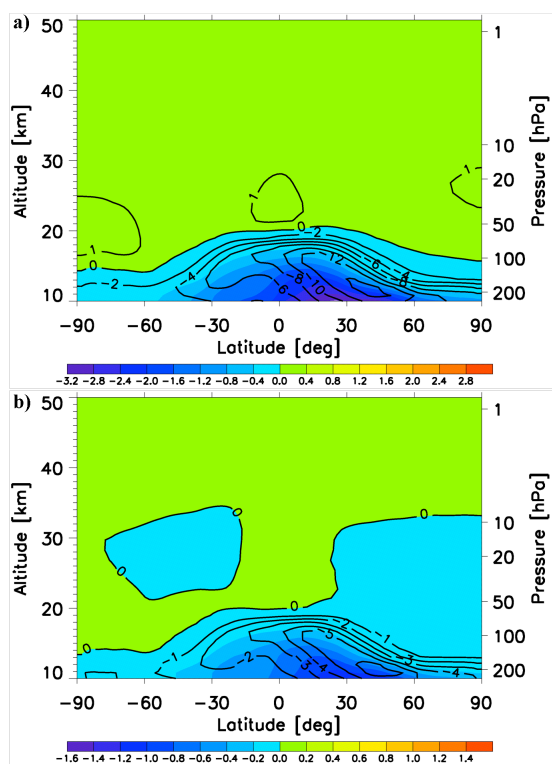


**Fig. 9.** Annually, zonally averaged HO<sub>x</sub> concentration changes in units of 10<sup>6</sup> molecules cm<sup>-3</sup> (shown by color) and the relative change in % (shown by contours) in the H<sub>2</sub>-ICE scenarios compared with the BL scenarios as a function of latitude and altitude for (a) A1FI and (b) B1 scenarios.

decrease in HO<sub>x</sub> concentrations (Fig. 9a) decreases the NO<sub>x</sub> loss due to Reaction (R1), which in turn increases NO<sub>x</sub>. In the middle stratosphere where HO<sub>x</sub> concentrations (Fig. 9a) are increased, the NO<sub>x</sub> loss due to Reaction (R1) is reduced, resulting in increased NO<sub>x</sub> concentrations. The maximum reduction, around 24 pptv, occurs at 35 km level near the Equator.

As shown in Fig. 11a, the ozone destruction rate due to HO<sub>x</sub> cycles at 35° N at the September equinox increases by 0.4 % to 1.1 % between 20 km and 50 km levels in the A1FI H<sub>2</sub>-ICE scenario, a direct result of increased HO<sub>x</sub> concentrations. In the middle stratosphere between 28 km and 40 km levels, the increase in the ozone destruction rate due to HO<sub>x</sub> cycles is more than 1 %. However, the contribution of HO<sub>x</sub> cycles to the total ozone destruction rate is the lowest in the middle atmosphere (Fig. 11b) because NO<sub>x</sub> cycles dominate ozone destruction here. In the upper and lower stratosphere where HO<sub>x</sub> cycles dominate, contributions of the HO<sub>x</sub> cycles to the total ozone loss rate increase by 0.35 % at 45 km level and by 0.3 % at 21 km level. This intensification is damped and even offset by the attenuation of the NO<sub>x</sub> cycles in the lower and middle stratosphere, resulting in reduction in total ozone loss rate between 23 and 30 km levels. The combined

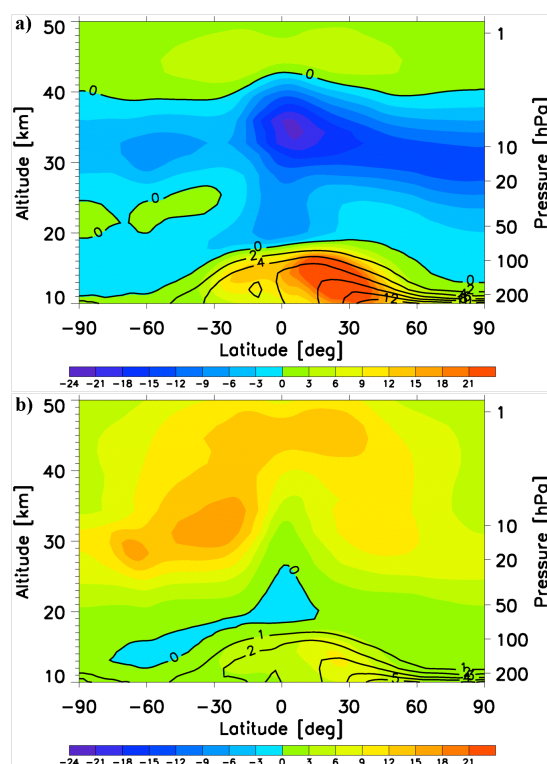


**Fig. 10.** Annually, zonally averaged NO<sub>x</sub> concentration changes in units of pptv (shown by color) and the relative change in % (shown by contours) in the H<sub>2</sub>-ICE scenarios compared with the BL scenarios as a function of latitude and altitude for (a) A1FI and (b) B1 scenarios.

impact of the perturbations to different catalytic cycles on ozone is small in magnitude but spatially widespread ozone concentration increases in the middle stratosphere (Fig. 8a). However, this increase does not fully compensate for the decrease in column in the lower stratosphere because ozone is denser in terms of molecular number concentration at lower levels. The global mean column ozone in the stratosphere would still be 0.23 % less than that in the A1FI BL atmosphere.

In the B1 H<sub>2</sub>-ICE scenario, the annual, global mean stratospheric column ozone is increased by 0.04 %, or 0.1 DU. Stratospheric column ozone is reduced north of 10° S but is increased south of this latitude throughout the year (Fig. 7b). The decrease in stratospheric column ozone in the Northern Hemisphere is no more than 0.5 DU. There is an increase of up to 3.5 DU, or 1 %, in stratospheric column ozone in the Antarctic region from October to December.

From the zonal mean perspective, annual mean ozone concentrations are reduced in the lower stratosphere in the B1 H<sub>2</sub>-ICE scenario (Fig. 8b). The reduction pattern resembles that of the A1FI H<sub>2</sub>-FC scenario, but the magnitude of reduction is much smaller. The maximum relative reduction (1.5 %) occurs at 17 km altitude, whereas the concentration

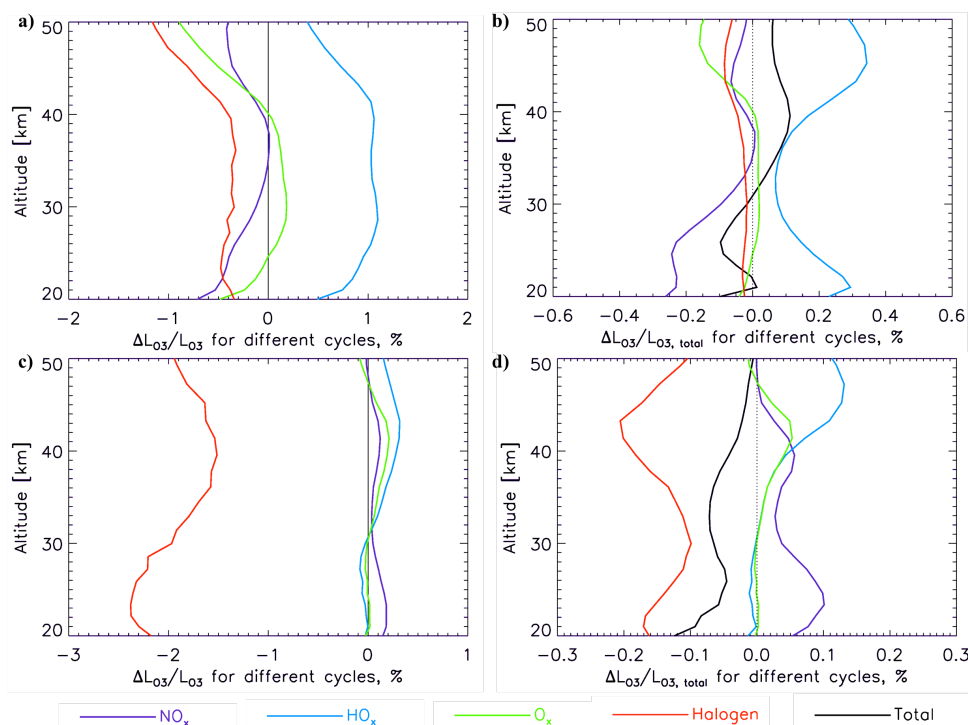


**Fig. 11.** Changes in contributions of different catalytic O<sub>3</sub> destruction cycles to the total O<sub>3</sub> loss in the H<sub>2</sub>-ICE scenarios compared to the baseline scenario. Panels (a) and (b) are for A1FI and panels (c) and (d) are for B1. (a) and (c) % change in contribution of each catalytic cycle compared to its contribution in the BL; (b) and (d) % change in contributions of different catalytic O<sub>3</sub> destruction cycles compared to the total O<sub>3</sub> loss rate in BL. All figures are daily averaged values for the September equinox at 35° N.

change is less than  $2 \times 10^{10}$  molecules cm<sup>-3</sup>. Ozone concentrations are increased in the rest of the stratosphere (except two cells of very slight reduction at 30 km level between 30° S and 60° S and between 30° N and 60° N). There is up to  $7 \times 10^{10}$  molecules cm<sup>-3</sup>,  $\sim 1\%$ , increase in ozone concentrations at levels around 18 km in the Antarctic region.

Again, HO<sub>x</sub> concentrations decrease in the troposphere in the B1 H<sub>2</sub>-ICE scenario, for the reason mentioned in discussion of the A1FI H<sub>2</sub>-ICE scenario. This decrease in the B1 H<sub>2</sub>-ICE scenario is smaller in magnitude compared with that in the A1FI H<sub>2</sub>-ICE scenario, but penetrates higher into the middle stratosphere (Fig. 9b), as the smaller strength of HO<sub>x</sub> source from the H<sub>2</sub> leakage emission in the B1 H<sub>2</sub>-ICE scenario cannot fully offset the decrease originated in the upper troposphere.

NO<sub>x</sub> concentrations increase in the whole stratosphere except for a small region in the Southern Hemisphere a few kilometers above the tropopause in the B1 H<sub>2</sub>-ICE scenario (Fig. 10b). In the lower stratosphere, NO<sub>x</sub> concentrations increase as they do in the A1FI H<sub>2</sub>-ICE scenario, but again the magnitude of increase is smaller. In the Southern Hemisphere, the changes of NO<sub>x</sub> concentrations are in the opposite sign to that of HO<sub>x</sub> concentrations (Fig. 9b), indicating a link between HO<sub>x</sub> and NO<sub>x</sub> concentrations via Reaction (R1). In the Northern Hemisphere, NO<sub>x</sub> concentrations increase as

a result of the widespread decrease in HO<sub>x</sub> concentrations (Fig. 9b). The increase in NO<sub>x</sub> concentrations in the middle and upper stratosphere can be as much as 20 ppbv; however, the perturbation to the NO<sub>x</sub> cycles is relatively small because the baseline NO<sub>x</sub> concentrations are high in this region.

In the stratosphere between 20 km and 50 km levels at 35° N at the September equinox, the perturbations to each catalytic cycle are modest (between  $-0.1\%$  and  $+0.3\%$ ) except for the halogen cycles, which decrease by 1.5% to 2.4% (Fig. 11c). Despite the NO<sub>x</sub> concentration increase (less than 1%) throughout the stratosphere, the impact of the enhanced NO<sub>x</sub> catalyzed cycles on ozone in the lower stratosphere is “buffered” by the decrease in the halogen catalyzed cycles (Fig. 11d). Increased NO<sub>x</sub> concentrations lead to slower halogen catalyzed cycles via halogen/NO<sub>x</sub> coupling, behaving like a buffer (Nevison et al., 1999). In the upper stratosphere, enhanced HO<sub>x</sub> catalyzed cycles are compensated for by decreased halogen catalytic cycles. The resulting ozone loss rate is slowed down throughout the stratosphere. Zonal mean ozone concentrations increase slightly throughout the middle and upper stratosphere (Fig. 11b). In the lower stratosphere, ozone decreases in the tropics and the Northern Hemisphere due to tropospheric impact, but increases in the southern high latitudes, where halogen catalyzed ozone loss cycles dominate, and halogen cycles are



slowed down in this region as NO<sub>x</sub> concentrations increase. In the B1 H<sub>2</sub>-ICE scenario, the overall impact on stratospheric column ozone is minimal (+0.04 %) among the studied H<sub>2</sub> scenarios.

## 5 Conclusions

In this study the possible impact of a future H<sub>2</sub>-based road transportation sector on stratospheric composition and chemistry was investigated through chemistry-climate model simulations of the 2050 atmosphere based on several emission scenarios designed to bracket the possible future changes in emissions. These scenarios are based on the IPCC high (A1FI) and low (B1) emitting paths. In addition, the impacts of two H<sub>2</sub> technology options are assessed: utilizing H<sub>2</sub> in fuel cells and utilizing H<sub>2</sub> in internal combustion engines.

The results of this study suggest that future implementation of a H<sub>2</sub>-based road transportation sector would perturb stratospheric chemistry by means of affecting catalytic ozone destruction cycles involving HO<sub>x</sub>, NO<sub>x</sub>, and halogens. The magnitude of the impact depends on the future growth path as well as the H<sub>2</sub> technology adopted. In general, the impact is larger for the A1FI based scenarios than for the corresponding B1 based scenarios, and the H<sub>2</sub>-FC scenarios result in more ozone loss than the H<sub>2</sub>-ICE scenarios. The impact on global stratospheric column ozone is considerable for the A1FI scenarios (−0.54 % for H<sub>2</sub>-FC and −0.23 % for H<sub>2</sub>-ICE) and for the B1 H<sub>2</sub>-FC scenario (−0.20 %), while there is a slight increase (0.04 %) for the B1 H<sub>2</sub>-ICE scenario. The largest relative reduction of ozone concentration occurs in the lower stratosphere where HO<sub>x</sub> cycles dominate O<sub>3</sub> loss and impact from the underlying troposphere is prominent. In the middle stratosphere, ozone concentrations increase slightly while at higher altitudes they either decrease slightly or increase slightly, depending on the scenario. These changes have relatively little impact on column ozone since ozone at this level only makes up a small fraction in terms of column ozone due to the low ozone number concentration there. It is important to note that the chosen emission scenarios are developed with a 100 % market penetration assumption. Less impact on stratospheric ozone is possible in cases of an intermediate market penetration.

It is important to note that even though a H<sub>2</sub>-based road transportation sector is likely to decrease stratospheric ozone, this reduction is considerably less than the ozone recovery due to the reductions in ozone depleting substances, e.g., CFCs, from the atmosphere in 2050. In terms of total column ozone, our results suggest that there would still be 4–5 % more ozone in the 2050 atmosphere with a H<sub>2</sub>-based road transportation sector than that in today's atmosphere. Therefore, the ozone reduction due to a H<sub>2</sub>-based road transportation sector should not constitute a major concern on stratospheric ozone and increased UV radiation at the earth's surface in 2050.

*Acknowledgements.* The authors thank Hugh Pitcher for providing projections of energy efficiency. Funding for this study was provided by the United States Department of Energy through award number DE-FC36-07GO17109 to the University of Illinois project "Evaluation of the Potential Environmental Impacts from Large-Scale Use and Production of Hydrogen in Energy and Transportation Applications". MKD would like to thank LANL's IGPP program for support.

Edited by: D. Shindell

## References

- Fleming, E. L., Jackman, C. H., Stolarski, R. S., and Douglass, A. R.: A model study of the impact of source gas changes on the stratosphere for 1850–2100, *Atmos. Chem. Phys.*, 11, 8515–8541, doi:10.5194/acp-11-8515-2011, 2011.
- Fuglestedt, J. S., Berntsen, T. K., Isaksen, I. S. A., Mao, H., Liang, X.-Z., and Wang, W.-C.: Climatic forcing of nitrogen oxides through changes in tropospheric ozone and methane: Global 3D model studies, *Atmos. Environ.*, 33, 961–977, 1999.
- Gettelman, A., Kinnison, D. E., Dunkerton, T. J., and Brasseur, G. P.: Impact of monsoon circulations on the upper troposphere and lower stratosphere, *J. Geophys. Res.*, 109, D22101, doi:10.1029/2004JD004878, 2004.
- Intergovernmental Panel on Climate Change (IPCC): Special Report on Emissions Scenarios. Working Group III, IPCC, Cambridge University Press, Cambridge, 2000.
- Jacobson, M. Z.: Effects of wind-powered hydrogen fuel cell vehicles on stratospheric ozone and global climate, *Geophys. Res. Lett.*, 35, L19803, doi:10.1029/2008GL035102, 2008.
- Kinnison, D. E., Brasseur, G. P., Walters, S., Garcia, R. R., Marsh, D. R., Sassi, F., Harvey, V. L., Randall, C. E., Emmons, L., Lamarque, J. F., Hess, P., Orlando, J. J., Tie, X. X., Randel, W., Pan, L. L., Gettelman, A., Granier, C., Diehl, T., Niemeier, U., and Simmons, A. J.: Sensitivity of chemical tracers to meteorological parameters in the MOZART-3 chemical transport model, *J. Geophys. Res.*, 112, D20302, doi:10.1029/2006JD007879, 2007.
- Ko, M. K. W., McElroy, M. B., Weisenstein, D. K., and Sze, N. D.: Lightning: a Possible Source of Stratospheric Odd Nitrogen, *J. Geophys. Res.*, 91, 5395–5404, 1986.
- Kulawik, S. S., Worden, H., Osterman, G., Luo, M., Beer, R., Kinnison, D. E., Bowman, K. W., Worden, J., Eldering, A., Lampel, M., Steck, T., and Rodgers, C. D.: TES atmospheric profile retrieval characterization: An orbit of simulated observations, *IEEE Trans. Geosci. Remote Sens.*, 44, 1324–1333, 2006.
- Lin, J. T., Patten, K. O., Hayhoe, K., Liang, X. Z., and Wuebbles, D. J.: Effects of future climate and biogenic emissions changes on surface ozone over the United States and China, *J. Appl. Met.*, 47, 1888–1909, 2008.
- Liu, C., Liu, Y., Cai, Z., Gao, S., Lu, D., and Kyrola, E.: A Madden-Julian Oscillation-triggered record ozone minimum over the Tibetan Plateau in December 2003 and its association with stratospheric "low-ozone pockets", *Geophys. Res. Lett.*, 36, L15830, doi:10.1029/2009GL039025, 2009.
- Liu, Y., Liu, C., Tie, X., and Gao, S.: Middle stratospheric polar vortex ozone budget during the warming Arctic winter, 2002–2003, *Adv. Atmos. Sci.*, 28, 985–996, 2011.

- Murphy, D. M., Fahey, D. W., Proffitt, M. H., Liu, S. C., Chan, K. R., Eubank, C. S., Kawa, S. R., and Kelly, K. K.: Reactive Nitrogen and its Correlation with Ozone in the Lower Stratosphere and Upper Troposphere, *J. Geophys. Res.*, 98, 8751–8773, 1993.
- Nevison, C. D., Solomon, S., and Gao, R. S.: Buffering interactions in the modeled response of stratospheric O<sub>3</sub> to increased NO<sub>x</sub> and HO<sub>x</sub>, *J. Geophys. Res.*, 104, 3741–3754, 1999.
- Pan, L. L., Wei, J. C., Kinnison, D. E., Garcia, R. R., Wuebbles, D. J., and Brasseur, G. P.: A set of diagnostics for evaluating chemistry-climate models in the extratropical tropopause region RID A-9296-2008, *J. Geophys. Res.*, 112, D09316, doi:10.1029/2006JD007792, 2007.
- Park, M., Randel, W., Kinnison, D., Garcia, R., and Choi, W.: Seasonal variation of methane, water vapor, and nitrogen oxides near the tropopause: Satellite observations and model simulations, *J. Geophys. Res.*, 109, D03302, doi:10.1029/2003JD003706, 2004.
- Sassi, F., Boville, B. A., Kinnison, D., and Garcia, R. R.: The effects of interactive ozone chemistry on simulations of the middle atmosphere, *Geophys. Res. Lett.*, 32, L07811, doi:10.1029/2004GL022131, 2005.
- Schultz, M. G., Diehl, T., Brasseur, G. P., and Zittel, W.: Air pollution and climate-forcing impacts of a global hydrogen economy, *Science*, 302, 624–627, 2003.
- Tromp, T. K., Shia, R. L., Allen, M., Eiler, J. M., and Yung, Y. L.: Potential environmental impact of a hydrogen economy on the stratosphere, *Science*, 300, 1740–1742, 2003.
- Wang, D., Jia, W., Olsen, S. C., Wuebbles, D. J., Dubey M. K., and Rockett, A. A.: Impact of a future H<sub>2</sub>-based road transportation sector on the composition and chemistry of the atmosphere – Part 1: Tropospheric composition and air quality, *Atmos. Chem. Phys.*, 13, 6117–6137, doi:10.5194/acp-13-6117-2013, 2013.
- Warwick, N. J., Bekki, S., Nisbet, E. G., and Pyle, J. A.: Impact of a hydrogen economy on the stratosphere and troposphere studied in a 2-D model, *Geophys. Res. Lett.*, 31, L05107, doi:10.1029/2003GL019224, 2004.
- Wennberg, P. O., Cohen, R. C., Stimpfle, R. M., Koplow, J. P., Anderson, J. G., Salawitch, R. J., Fahey, D. W., Woodbridge, E. L., Keim, E. R., Gao, R. S., Webster, C. R., May, R. D., Toohey, D. W., Avallone, L. M., Proffitt, M. H., Loewenstein, M., Podolske, J. R., Chan, K. R., and Wofsy, S. C.: Removal of Stratospheric O<sub>3</sub> by Radicals: In-Situ Measurements of OH, HO<sub>2</sub>, NO, NO<sub>2</sub>, ClO, and BrO, *Science*, 266, 398–404, 1994.
- World Meteorological Organization (WMO): Scientific Assessment of Ozone Depletion: 1994, WMO Rep.37, Geneva, 1995.
- World Meteorological Organization (WMO): Scientific Assessment of Ozone Depletion: 2002, WMO Rep.47, Geneva, 2003.
- World Meteorological Organization (WMO): Scientific Assessment of Ozone Depletion: 2010, WMO Rep.52, Geneva, 2011.
- Wu, S., Mickle, L. J., Jacob, D. J., Rind, D., and Streets, D. G.: Effects of 2000–2050 changes in climate and emissions on global tropospheric ozone and the policy-relevant background surface ozone in the United States, *J. Geophys. Res.*, 113, D18312, doi:10.1029/2007JD009639, 2008.
- Wuebbles, D. J and Hayhoe, K.: Non-CO<sub>2</sub> Greenhouse Gases: Scientific Understanding, Control and Implementation, 425–432, edited by: van Ham, J., Baede, A. P. M., Meyer, L. A., and Ybema, R., Kluwer Academic Publishers, 2000.